SILICA ACTIVITY AND RAMAN SPECTRA OF THE CaO-SiO$_2$-TiO$_x$ SYSTEM

G. Tranell, O. Ostrovski[*] and S. Jahanshahi[**]

SINTEF Materials Technology, N-7465 Trondheim, Norway

[*]School of Materials Science and Engineering, The University of New South Wales, Sydney, NSW 2052, Australia

[**]GK Williams CRC for Extractive Metallurgy, CSIRO Minerals, Victoria, Australia

ABSTRACT

The thermodynamic activity of SiO_2 in CaO-SiO_2-TiO_x slags was measured by the slag-metal-gas equilibrium method. Slags containing up to 43 mol% TiO_x, were equilibrated with molten copper in molybdenum crucibles in H_2-H_2O-Ar gas atmosphere. The oxygen partial pressure and temperature were maintained at ~10^{-12} atm and 1873 K, respectively. In the equilibrated slags, the proportion of titanium in the reduced Ti^{3+} state ranged from 16% to 54% of total Ti by mass. Results showed that at a given CaO/SiO_2 ratio, the activity coefficient of SiO_2 increases with increasing TiO_x concentration.

Samples of CaO-SiO_2-TiO_x slags were also examined by Raman spectroscopy. Raman spectra obtained for oxidised and reduced CaO-SiO_2-TiO_x slags show that the Ti^{4+} ion has a tetrahedral coordination, while the coordination of Ti^{3+} appears to be predominantly octahedral. These findings are consistent with the observed effect of titania on the silica activity in the CaO-SiO_2-TiO_x slags.

I. INTRODUCTION

Raman spectroscopic studies showing that the Ti^{4+} ion in silicate melts has tetrahedral coordination has led to the assumption that the Ti^{4+} is a net-forming ion[1-3]. The Ti^{4+} ion has also demonstrated glass-forming properties[4]. These findings are supported by the thermodynamic studies of Martin *et al.*[5] and Matsuzaki and Ito[6], which showed that silica and titania generally compete for coordination with basic components such as CaO, MnO and FeO. Studies of thermodynamic properties of TiO_2-CaO, TiO_2-MnO and TiO_2-FeO solutions[7-12] showed negative deviation of these systems from the ideal solutions. However, addition of titania to silicate slag decreases its viscosity and increase electrical conductivity and sulfide capacity[13-15], which can be interpreted as a weakening of the silicate network. On this basis, titanium dioxide is classified as an amphoteric oxide[16].

Titanium oxides Ti_2O_3 and TiO are generally regarded as basic oxides. The coordination of the Ti^{3+} ion in reduced slags is predominantly considered octahedral.[17]

Some properties of titanium-containing slags are strongly dependent on the partitioning of titanium between different valency states. Distribution of titanium between Ti^{3+} and Ti^{4+} valency states in the CaO-SiO_2-TiO_x system has recently been studied by the present authors[18-19]. These and other published studies[20,21] on redox equilibria in titania slags have established that proportion of titanium in the reduced Ti^{3+} valency state increases with

increasing temperature and decreasing oxygen potential and CaO/SiO_2 ratio. These findings were supported by a study of the thermodynamic properties of complex blast furnace slags, carried out by Morizane and co-workers[22].

The effect of titania on silica activity in the $CaO-SiO_2-TiO_2$ system was recently examined by the Knudsen mass spectrometric method[23]. For melts with constant mole fraction of SiO_2, it was found that the SiO_2 activity increased with increasing TiO_2 concentration.

This paper presents results on silica activity measurements in the $CaO-SiO_2-TiO_x$ system, with a relatively high proportion of titanium present in the reduced Ti^{3+} state, using a metal-slag-gas equilibrium method. The thermodynamic properties of a silicate slag depend strongly on the silicate structure. This paper also reports on the silicate-titanate structure of $CaO-SiO_2-TiO_x$ slags obtained under oxidising and reducing conditions, as studied by Raman spectroscopy.

II. EXPERIMENTAL

A. Measurement of Silica Activity

Activity of silica in the $CaO-SiO_2-TiO_x$ system was measured by the metal-slag-gas equilibrium method. 15 g of chemically pure copper (>99.999%) and 4 g of master slag powder were placed in a molybdenum crucible. The compositions of the 14 different $CaO-SiO_2-TiO_2$ master slags used in the study, prepared through a repeated melting and grinding procedure[18-19], are specified in Table I.

The reducing gas atmosphere in the two main series of metal-slag-gas experiments was made up by mixing hydrogen, water vapour and argon. Both the argon and hydrogen gases were purified by passing them through silica gel to remove moisture. Argon was deoxidized by passing it over copper- turnings heated to 873 K. A preliminary series of experiments was also carried out in a $CO-CO_2-Ar$ gas atmosphere, made from a premixed CO/CO_2 gas mixture and argon.

All experiments were performed at 1873 K under an oxygen potential of 10^{-12} atm, in a vertical tube furnace fitted with end-caps allowing the atmosphere to be controlled. Experiments at lower oxygen partial pressure could bring significant losses of silica from the slag phase. This was observed by Sakai and Suito[24] in experiments conducted at oxygen potential below $10^{-12.5}$ atm. The water vapour-hydrogen ratio in the gas mixture required to obtain the desired oxygen potential was calculated from the equilibrium constant of reaction (1) using data of Kubachewski and Alcock[25].

$$H_2 + \tfrac{1}{2}O_2 = H_2O \qquad [1]$$

$$\ln K_1 = \frac{29641.3}{T} - 6.59$$

The targeted water vapour pressure was obtained by the following method described by Gokcen[26]. The purified hydrogen was passed through three sets of glass bubbler bottles containing a saturated lithium chloride water solution. The bottles were immersed in a temperature controlled water bath. The moisture content in the reaction gas obtained at different temperatures was also analysed by a calibrated Fison VG Prima 600, scanning

magnetic sector mass spectrometer. The mass-spectrometric results in comparison with calculated water vapour pressure using data[26] are shown in Figure 1. Measured water vapour pressures were slightly higher than those determined by Gokcen[26].

The hydrogen-water vapour mixture generated over the lithium chloride solution after exiting the last bubbler bottle was immediately mixed with argon. The gas flow ratio of hydrogen-water to argon was approximately 1:9. This kept the total moisture content of the reaction gas very low and avoided water condensation. The total reaction gas flow rate was approximately 0.7 l/min.

The equilibrium experiments were carried out in a vertical $MoSi_2$ tube furnace fitted with water-cooled brass end caps, enclosing an alumina working tube. The crucible was suspended from an alumina gas delivery tube and initially held in the cool part of the furnace tube whilst purging the working tube with argon. After approximately 30 minutes, the crucible was lowered into the hot zone and the reducing gas was added to the gas stream. When the sample had reached equilibrium, the reducing gas was turned off and the reaction tube rapidly flushed with argon due to the explosive nature of the gas, before the sample was withdrawn from the furnace and quenched in water.

The equilibrated copper and slag phases were separated from the molybdenum crucible by machining on a lathing the crucible bottom and walls off to the depth of the copper-slag interface. The copper button was subsequently cut off with a silicon carbide blade and the slag removed from the crucible.

The compositions of the outlet gases from the furnace were determined on-line with the mass spectrometer throughout the experiments. The oxygen partial pressure of the reaction gas was determined from the mass spectrometric measurements of water vapour and hydrogen pressure.

The mass spectrometer was calibrated for hydrogen and argon using standard gases, as recommended by the supplier. The calibration for moisture content was done using air of a known temperature and moisture content, measured by a Panametrics high temperature relative humidity transmitter. The absolute accuracy of measurements of argon and hydrogen gas concentrations were approximately $<\pm 0.01$ and $<\pm 0.1$ volume percent respectively. The accuracy of the moisture measurement was approximately $<\pm 2$ percent of the measured value.

The minimum time needed to achieve equilibrium between the copper, slag and gas phases, was determined through reduction kinetic experiments for slag 12 (a high TiO_x concentration and low basicity slag). In these experiments, the Ti^{3+}/Ti^{4+} ratio and silicon concentration in copper were determined as a function of reaction time. The results showed that 24 hours was sufficient to achieve equilibrium between the metal, slag and gas phases.

The fraction of titanium in the reduced Ti^{3+} state in the equilibrated slags was determined using an indirect potentiometric redox titration method, as described in earlier publications[18-19]. The slags were also analysed for minor components such as Cu and Mo, using X-ray Fluorescence.

The copper buttons after reduction experiments were machined and polished clean on one side and subsequently analysed for concentrations of molybdenum, silicon and titanium in a VG9000 Glow Discharge Mass Spectrometer (GDMS)[27]. The detection limits for all three elements were typically at parts per billion (by weight) levels. The relative errors quoted for

molybdenum, silicon and titanium concentrations in copper were 5 percent on concentrations in the ppm range. In the sub-ppm levels, uncertainties were estimated at 30 percent. As a reference, an un-reacted sample of the pure copper was analysed.

In addition to GDMS analysis, copper samples were also analysed for molybdenum, silicon and titanium, using ICP-AES. The samples were prepared by dissolving drilled copper turnings by a standard procedure. The error of measurement of the molybdenum and silicon concentrations is quoted to be around 2 percent. The minimum detection level for titanium was 0.5 parts per million. However, both the GDMS and ICP-AES techniques yielded poor results for titanium in copper.

B. Raman Spectroscopy

Changes in structure due to changes in oxygen potential were investigated by Raman spectroscopy. The quenched equilibrated slags and the master slags (pre-melted in air) were investigated. Raman spectra of pieces of slags were taken using a Renishaw Raman Microscope 2000, with a helium laser (wave no. 6.14). The slag samples were scanned over the Raman shift interval 100 to 1500 cm^{-1}, for 20 seconds. The samples investigated by the Raman spectroscopy had CaO/SiO_2 ratio of ~1.25 and different TiO_x concentrations (Slags No: 1, 5 and 9). The reduced samples were obtained at 1873 K and $p_{O2} = 10^{-12}$ atm and the oxidised samples came from masters slags which were pre-melted in air and quenched.

III. RESULTS AND DISCUSSION

A. Silica activity in the CaO-SiO_2-TiO_x system

Results of the equilibrium experiment series are presented in Tables II to IV.

As seen from Table II, measured molybdenum concentrations in the equilibrated copper rarely exceeded 200 ppm and showed no effect on the interpreted results. In the equilibrated slag, concentrations of copper and molybdenum were also low (Table II).

The concentrations of titanium in copper were extremely inconsistent (Tables II-IV) due to very low titanium content. These results were disregarded from further discussion. Concentrations of silicon in copper were several orders of magnitude higher than those determined for titanium and were reasonably consistent. The relative error of measurements of silicon content in copper was estimated to be ±30%.

The activity of SiO_2 in a slag was be determined using the equilibrium constant K_2 for reaction (2) as follows.

$$SiO_2(s) \leftrightarrow \underline{Si} + O_2(g) \tag{2}$$

$$a_{SiO_2} = \frac{g_{Si} X_{Si} \times p_{O_2}}{K_{[2]}} \tag{3}$$

Where; γ_{Si} is the activity coefficient for silicon in copper and X_{Si} is the equilibrium concentration of silicon in liquid copper.

The equilibrium constant $K_{[2]}$ was calculated from the standard Gibbs free energy for reaction (2)[25]:

$$\Delta G^{\circ}_{[2]} = 952{,}697 - 203.8T \qquad \text{(J/mole)}$$

The silicon concentration in copper obtained in the equilibrium experiments was rather low, and the copper-silicon solution was considered to be dilute with respect to silicon. The activity coefficient of silicon in copper at 1873 K was estimated to 0.018, based on results of copper-gas-pure silica equilibrium experiment and literature data[28].

The determined silica activities in the $CaO\text{-}SiO_2\text{-}TiO_x$ system are plotted against mole fraction SiO_2 in Figure 2. This Figure also presents silica activity in the $CaO\text{-}SiO_2\text{-}TiO_2$ measured by the Knudsen effusion method[23]. Slags from the slag-metal-gas experiments were equilibrated under strongly reducing conditions and contained substantial concentration of $TiO_{1.5}$ (the Ti^{3+}/Ti^{4+} ratio ranged from 0.3 to 0.6). The titanium redox state in the samples examined by the Knudsen effusion method was mainly in the form of TiO_2. Activity of silica in the reduced $CaO\text{-}SiO_2\text{-}TiO_x$ slags is generally lower than that in the $CaO\text{-}SiO_2\text{-}TiO_x$ system. This implies that reduced $CaO\text{-}SiO_2\text{-}TiO_x$ slags are more basic than the $CaO\text{-}SiO_2\text{-}TiO_2$ slags.

The silica activities in the $CaO\text{-}SiO_2\text{-}TiO_x$ system are plotted in Figure 3. The silica activities in the $CaO\text{-}SiO_2$ binary system were taken from the system optimisation of Eriksson *et al.*[29], which are in close agreement with the generally accepted, experimentally measured values of Kay and Taylor[30]. As seen from Fig. 2, SiO_2 activities in the $CaO\text{-}SiO_2\text{-}TiO_x$ system containing up to 17 mol% TiO_x, generally exhibit the same behaviour as the $CaO\text{-}SiO_2$ system. That is negative deviation from ideality at SiO_2 mole fractions below 0.5-0.55. Above SiO_2 mole fractions of 0.5-0.55, the deviation from ideality is positive.

In both oxidised and reduced $CaO\text{-}SiO_2\text{-}TiO_x$ slags, at a constant mole fraction of silica the activity of SiO_2 increases with increasing TiO_x content. This is expected, given the difference in basicity of TiO_x and CaO.

B. *Raman Spectra and Structure of $CaO\text{-}SiO_2\text{-}TiO_x$ slags*

The Raman spectra of $CaO\text{-}SiO_2$ and $CaO\text{-}SiO_2\text{-}TiO_x$ slags are shown in Figures 4 to 7.

Following Mysen *et al*[2] and Furukawa and White[1], main peaks in the Raman spectrum of a titanium-free $CaO\text{-}SiO_2$ slag with a CaO/SiO_2 ratio of 1.25, are associated with $Si_2O_5^{2-}$ sheets (band near 1070 cm^{-1}), $Si_2O_6^{4-}$ chains (peak around 950cm^{-1}) and depolymerised SiO_4^{4-} (band near 850 cm^{-1}). The band between 600 and 660 cm^{-1} and the shoulder around 340 cm^{-1}, are caused by O-Si-O deformation motions in the imperfect network. Addition of TiO_x to calcium silicate changes positions and intensities of main peaks associated with silicate structural units and also introduces new peaks in the Raman spectra.

Effects of TiO_2 on the Raman spectra of $CaO\text{-}SiO_2\text{-}TiO_2$ samples (oxidised slag, Figures 5a, 6a and 7a) can be summarised as:

1. Positions of the main 850 cm^{-1} and 950 cm^{-1} peaks, associated with Si^{4+} monomers and chains, remain virtually unchanged, although their heights, and therefore, relative

concentrations of monomers and chains are affected. The peak at 1070 cm^{-1} in titanium-free slags, indicative of silicate sheets, is displaced to a position between 1000 and 1030 cm^{-1}.

2. The intensity of the peak between 1020 and 1030 cm^{-1} increases while the intensity of the peak at 950cm^{-1} decreases with increasing titanium content of the slag. The intensity of the peak located at 850 cm^{-1} decreases slightly with the introduction of 14 wt% titanium; with further addition of TiO_2 up to 21 wt%, the intensity of this peak increases rapidly.

3. A new peak appears in the band of 750 to 800 cm^{-1}. Its intensity increases with increasing TiO_2 concentration.

4. The band around 660 cm^{-1}, associated with oxygen deformation motion, exists only in melts with low titanium concentrations and then disappears. The shoulder located around 340 cm^{-1} remains.

The Raman spectra of the oxidised $CaO\text{-}SiO_2\text{-}TiO_2$ slags can be interpreted as follows:

(1) Furukawa and White[1], and by Mysen *et al.*[2] in their study of the Raman spectra of crystallised titanates with Ti^{4+} in six-fold co-ordination observed stretch bands only below ~650cm^{-1}. Given that no new peaks appeared in the spectra of the $CaO\text{-}SiO_2\text{-}TiO_2$ slags below 650 cm^{-1}, it is reasonable to assume that the coordination of Ti^{4+} is mainly tetrahedral.

(2) The band between 1000 and 1030cm^{-1} is interpreted as resulting from (Si,Ti) coupling of stretch vibrations in a sheet unit with randomly distributed Ti^{4+} and Si^{4+} [2]. The increasing intensity of this peak with increasing TiO_2 concentration indicates that the proportion of the $(Si,Ti)_2O_5^{2-}$ units increases relative to other units. The slight shift towards lower frequencies indicates that the unit becomes more titanium rich as the TiO_2 concentration increases.

(3) With an increasing addition of TiO_2, the intensity of the peak located around 950cm^{-1}, associated with $Si_2O_6^{4-}$ chain units, decreases markedly. This decrease is related to the overall decrease of SiO_2 concentration in the melt and is also a reflection of the effect of TiO_2 on the partitioning of SiO_2 between different silicate structural units. The peak around 850cm^{-1}, associated with de-polymerised Si^{4+} units, generally increases in intensity as the titanium concentration increases. This peak also reflects the presence of $Ti_2O_6^{4-}$ chain units (in accordance with Mysen *et al.* [2] this peak is located at ~880 cm^{-1}). Thus, the increasing intensity of this peak is due to both the appearance of the $Ti_2O_6^{4-}$ chain and the shift in silica structural units partitioning towards de-polymerised units. In slags containing 21 wt% TiO_2, silicate monomers, titanate chains and (Si,Ti)-sheets are the predominant structural units.

(4) As the titanium concentration increases, the peak between 750 and 800 cm^{-1}, becomes more pronounced. This trend may be interpreted as an increased proportion of depolymerised TiO_4^{4-} monomers[1-2].

Thus, the four-fold Ti^{4+} ion exists in monomer, chain and Si-coupled sheet units. The equilibrium between these titanate units can be presented as:

$$3Ti_2O_6^{4-}(chain) = 2TiO_4^{4-}(monomer) + 2Ti_2O_5^{2-}(sheet) \quad (5)$$

In samples with 7 and 14wt% TiO_2, the predominant structural Ti^{4+} is TiO_4^{4-}. In the sample with 21 wt% TiO_2, the $Ti_2O_6^{4-}$ is likely to be the main structural unit.

Relationship between concentrations of titanate and silicate structural units may be presented by reaction (6), which reflects experimental observation of the competition of the titanate and silicate units to coordinate with the Ca^{2+} ion[2].

(Si-O-Ca-O-Si) + (Ti-O-Ti) = (Si-O-Si) + (Ti-O-Ca-O-Ti) (6)

Following the equilibrium constant for reaction (6), in a slag of a given CaO/SiO_2 ratio, a decrease in the fraction of silicate complexes would occur in favour of titanate complexes and depolymerised silica units (monomers). An addition of TiO_2 to a molten silicate with no free O^{2-} alters the ratio between polymerised and de-polymerised silicate units.

Changes in the Raman spectra of the $CaO\text{-}SiO_2$ system with addition of TiO_2 and major changes in the Raman spectra of the $CaO\text{-}SiO_2\text{-}TiO_2$ slags with increasing TiO_2 concentration take place in the high frequency envelope. No new peaks appear in the low frequency envelope of the spectra. The relative intensity of the shoulder around 340 cm^{-1} increases slightly compared to the main peak as the titanium concentration increases. This may be caused by additional "defects" or "deformations" in the structure with the presence of tetrahedral Ti^{4+}.

The $CaO\text{-}SiO_2\text{-}TiO_x$ samples equilibrated at 1873 K under reducing conditions with oxygen partial pressure in the gas phase of 10^{-12} atm, contained a significant fraction of titanium in the reduced Ti^{3+} state. In samples containing 7, 14 and 21 wt% TiO_x (CaO/SiO_2~1.25), the Ti^{3+}/Ti^{4+} ratios were found to be 0.19, 0.12 and 0.17, respectively.

In accordance with work of Iwamoto *et al.* [17], Ti^{3+} in silicate melts has an octahedral coordination. Therefore, no new peaks are expected in the high frequency envelope of the Raman spectra of the $CaO\text{-}SiO_2\text{-}TiO_x$ slags containing Ti^{3+}, and this was confirmed by the present study. Partial reduction of TiO_2 to $TiO_{1.5}$ does not change the general pattern of the Raman spectra. As seen in Figures 5b to 7b, the main peaks retain their positions in the bands of 650-700 cm^{-1}, 750-800 cm^{-1}, 850-880 cm^{-1}, 950-980 cm^{-1} and 1000-1050 cm^{-1}. This indicates that structural units associated with Ti^{4+} and Si^{4+} in the oxidised and reduced samples are the same, namely $(Si,Ti)_2O_5^{2-}$ sheet units (peak at ~1030 cm^{-1}), $Si_2O_6^{4-}$ and $Ti_2O_6^{4-}$ chain units (peaks at 950 cm^{-1} and ~880 cm^{-1}) and SiO_4^{4-} and TiO_4^{4-} depolymerised units (peaks near 850 cm^{-1} and 750-800 cm^{-1}, respectively).

While the overall shape of the high frequency envelopes remained unchanged, the presence of titanium in the reduced Ti^{3+} valency state affected proportions of structural units. The most noticeable difference between the spectra of reduced and oxidised slags was observed for the peak around 950 cm^{-1}, associated with silicate chain units. The relative intensity of this peak was consistently higher in slags equilibrated under reducing conditions. This indicates that the Ti^{3+} content increases the relative proportion of Si^{4+} present in silicate chains. This observation is in accord with results obtained for oxidised slags, where all the Ti is in the Ti^{4+} oxidation state: with increasing concentration of TiO_2 in the $CaO\text{-}SiO_2\text{-}TiO_2$ slags, the intensity of the 950 cm^{-1} peak associated with $Si_2O_6^{4-}$ chain units, decreases markedly. Decreasing the Ti^{4+}/Ti^{3+} redox ratio decreases the total Ti^{4+} concentration in the $CaO\text{-}SiO_2\text{-}TiO_2$ system and there is a corresponding increase in the intensity of the 950 cm^{-1} peak.

The Raman spectra of the $CaO-SiO_2-TiO_2$ system are in accord with results on the effect of titania on the silica activity. The Ti^{4+} ion, having tetrahedral coordination, acts acidic (net-forming) and its addition to the $CaO-SiO_2-TiO_x$ slag increases silica activity. Titanium in the reduced Ti^{3+} valency state has octahedral coordination and behaves as a basic oxide. Lowering the Ti^{4+}/Ti^{3+} redox ratio decreases the silica activity.

IV. CONCLUSIONS

The findings from the study of thermodynamic activity of silica and Raman spectra of $CaO-SiO_2-TiO_x$ slags can be summarized as follows:

- The activity of SiO_2 in $CaO-SiO_2-TiO_x$ slags containing up to 17 mol% TiO_x, exhibits negative deviation from ideality at SiO_2 mole fractions below 0.50-0.55 and positive deviation at higher silica contents.

- At a constant silica concentration, the activity of SiO_2 in calcium silicate based melts increased with increasing TiO_x concentration between 5 and 17 mol%.

- In $CaO-SiO_2-TiO_x$ slags, containing significant proportion of $TiO_{1.5}$, the activity of SiO_2 is lower than in oxidised slags containing titanium predominantly as TiO_2.

- Consistent with observations made in other published studies; Ti^{4+} in oxidized $CaO-SiO_2-TiO_2$ slags has four-fold coordination and forms similar structural units to Si^{4+}, that is monomers and chains. Ti^{4+} is also present in Si, Ti coupled sheet units.

- Introduction of TiO_2 to $CaO-SiO_2$ system alters the equilibrium between de-polymerised and polymerised silicate structural units. Adding titanium oxide to the $CaO-SiO_2$ slags decreases the fraction of polymerised silicate units and increases the fraction of polymerised titanate units.

- The coordination of Ti^{4+} ion, as well as the structural Si^{4+} and Ti^{4+} units in $CaO-SiO_2-TiO_2-TiO_{1.5}$ slags are the same as in the $CaO-SiO_2-TiO_2$ slags.

- Decreasing the Ti^{4+}/Ti^{3+} ratio increases the fraction of Si^{4+} in chain units relative to that in monomers and sheet units. This confirms that Ti^{3+} can be regarded as a basic species.

ACKNOWLEDGMENTS

Financial support for this work was provided by the Australian Research Council and the Australian Government Co-operative Research Centres Program through G K Williams Cooperative Research Centre for Extractive Metallurgy, a joint venture between the CSIRO Minerals and the Department of Chemical Engineering, the University of Melbourne.

The authors gratefully acknowledge the co-operation with the Knudsen Mass-Spectrometry group at the University of St. Petersburgh, Russia – V.L. Stolyarova and co-workers.

REFERENCES

1. T. Furukawa and W.B. White; *Physics and Chemistry of Glasses*, 1979, vol. 20, pp. 69-80.
2. B.O. Mysen, F.J. Ryerson and D. Virgo; *American Mineralogist*, 1980, vol. 65, pp. 1150-1165.
3. R.B. Greegor, F.W. Lytle, D.R. Sandstrom, J. Wong and P. Schultz; *Journal of Non-Crystalline Solids*, 1983, vol. 55, pp. 27-43.
4. B.V.J Rao; *Journal of the American Ceramic Society*, 1964, vol. 47, pp. 455-463.
5. E. Martin, O.I.H Abdelkarim, I.D Sommerville and H.B Bell; *Metal-Slag-Gas Reactions and Processes*, Toronto, Electrochemical Society, 1975, pp. 1-7.
6. K. Matzusaki and K. Ito; *ISIJ International*, 1997, vol. 37, pp. 562-565.
7. S. Banon, C. Chatillon and M. Allibert; *Canadian Metallurgical Quarterly*, 1981, vol. 20, pp. 79-84.
8. S. Banon, C. Chatillon and M. Allibert; *High Temperature Science*, 1982, vol. 15, pp. 105-128.
9. E. Martin and H.B. Bell; *Transactions of the Institute of Mining and Metallurgy*, 1974, vol. 83, pp. C193.
10. I.C. Smith and H.B. Bell; *Transactions of the Institution of Mining and Metallurgy*, 1970, vol. 79, pp. C253-258.
11. S. Ban-ya, A. Chiba and A. Hikosaka; *Tetsu-to-Hagane*, 1980, vol. 66, pp. 1484-1493.
12. B.K.D.P. Rao and D.R. Gaskell; *Metallurgical Transactions B*, 1981, vol. 12B, pp. 469-477.
13. H. Schenck and M.G. Frohberg; *Archiv fur das Eisenhuttenwesen*, 1962, vol. 33, pp. 421-425.
14. K. Morinaga, Y. Suginohara and T. Yanagase; *Tetsu-to-Hagane*, 1974, vol. 38, pp. 658-662.
15. S.D. Brown, R.J. Roxburgh, I. Ghita and H.B. Bell; *Iron and Steelmaking*, 1982, vol. 9, pp. 163-167.
16. I.D. Sommerville and H.B. Bell; *Canadian Metallurgical Quarterly*, 1982, vol. 21, pp. 45-155.
17. N. Iwamoto, H. Hidaka and Y. Makino; *Journal of Non-Crystalline Solids*, 1983, vol. 58, pp. 131-141.
18. G. Tranell, O. Ostrovski and S. Jahanshahi, *Proceedings of the 5th International Conference on Molten Slags, Fluxes and Salts, ISS*, Warrendale, PA, 1997, pp. 152-161.
19. G. Tranell; Ph.D Thesis, The University of New South Wales, Sydney, Australia, 1999
20. J. Tanabe and H. Suito; *Steel Research*, 1992, vol. 63, pp. 515-520.
21. H.D. Schreiber, T. Thanyasiri, J.J Lach and R.A. Laegere; Physics and Chemistry of Glasses, 1978, vol. 19, pp. 126-139.

22. Y. Morizane, B Ozturk and R.J. Fruehan; *Metallurgical and Materials Transactions B*, 1999, vol. 30B, pp. 29-43.

23. O. Ostrovski *et al.*; *High Temperature Materials and Processes*, 2000, In Print.

24. H. Sakai and H. Suito; *ISIJ International*, 1996, vol. 36, pp. 143-149.

25. O. Kubachewski and C.B. Alcock; "Metallurgical Thermochemistry", 5th edition, *Pergamon Press*, 1989.

26. N.A. Gokcen; *Journal of the American Chemical Society*, 1951, vol. 73, pp. 3789-3790.

27. D.M.P. Milton, R.C. Hutton and G.A. Ronan; *Fresenius Journal of Analytical Chemistry*, 1992, vol. 343, pp. 773-777.

28. P.J. Bowles H.F. Ramstad and F.D. Richardson, F.D; *Journal of the Iron and Steel Institute*, 1964, pp. 113-121.

29. G. Eriksson, P. Wu, M. Blander and A.D. Pelton; *Canadian Metallurgical Quarterly*, 1994, vol. 33, 1, pp. 13-21.

30. D.A.R. Kay and J. Taylor; *Transactions of the Faraday Society*, 1960, vol. 56, pp. 1372-1375

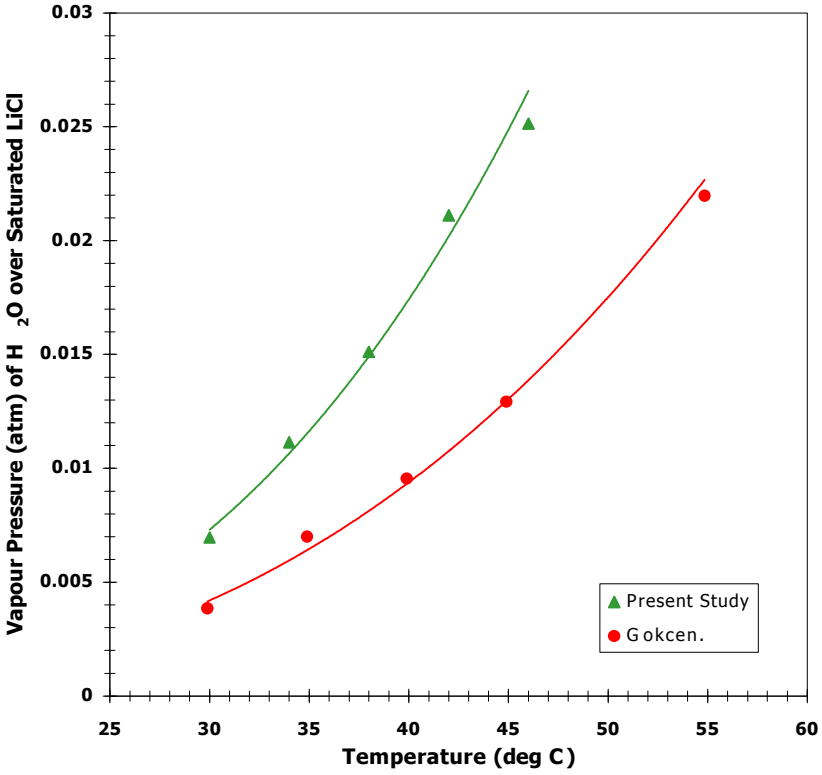

Figure 1: Water vapour pressure over saturated lithium chloride for a range of water bath temperatures, as measured by mass spectrometer. Results compared with those of Gokcen[26].

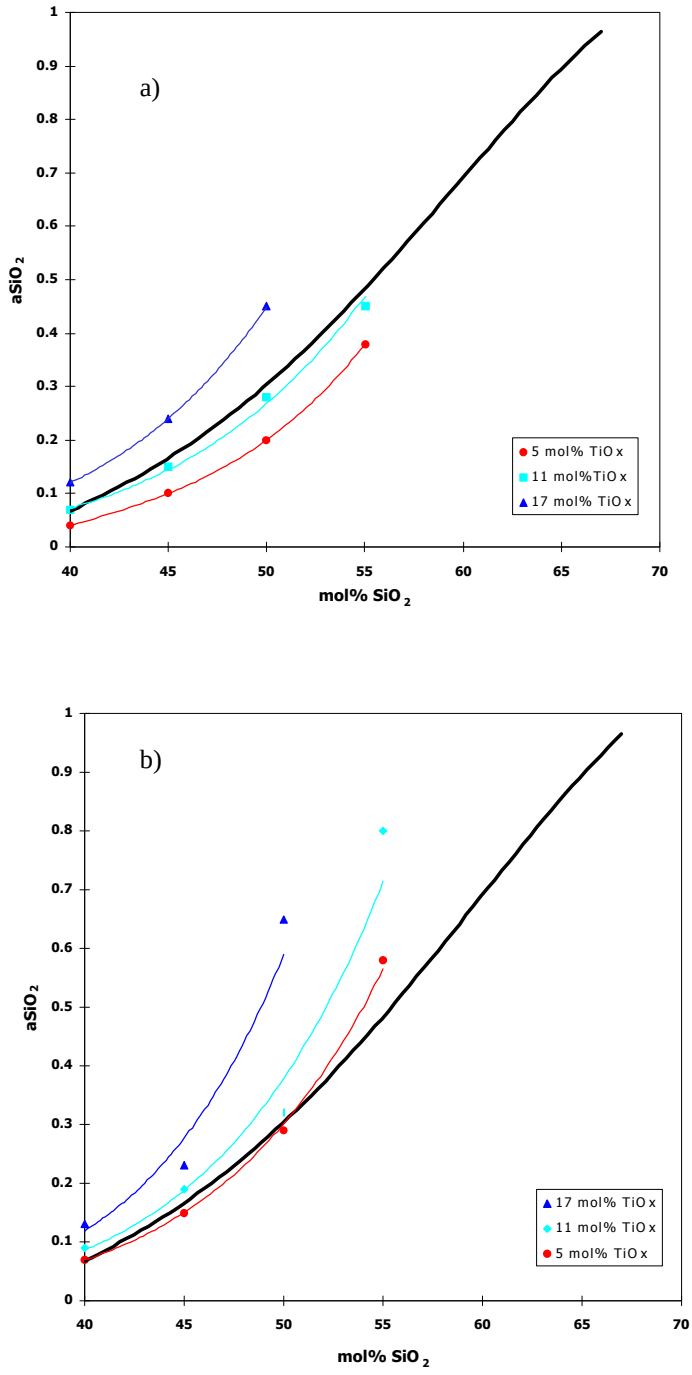

Figure 2: Activity of silica as a function of silica mole fraction in CaO-SiO_2-TiO_x slags at **a)** 1873 K and oxygen potential 10^{-12} atm, as measured by the metal-slag-gas equilibrium technique (Solid SiO_2 (crist.) standard state). NB! Points estimated from iso-activity lines in Figure 3. **b)** 1850 K and oxygen potential ~10^{-9} atm (Solid SiO_2 (crist.) standard state), measured by Stolyarova *et al.*[23] through the Knudsen effusion method.. The black line denotes the silica activity in the CaO-SiO_2 binary system, after Eriksson *et al.*[29].

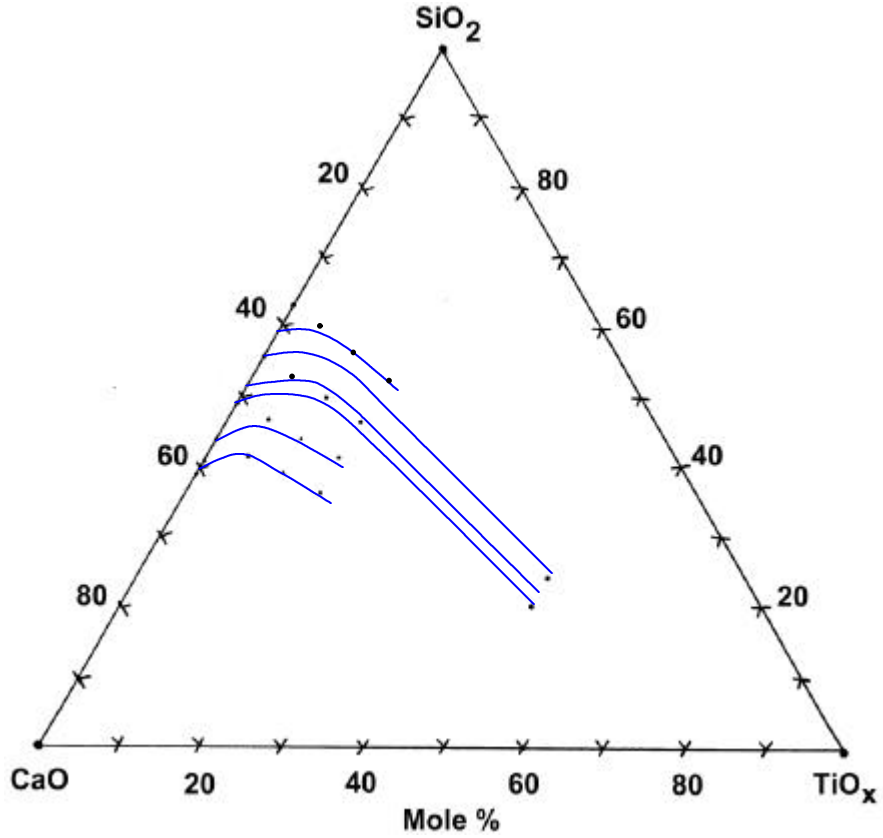

Figure 3: Approximate SiO_2 iso-activity curves in the $CaO\text{-}SiO_2\text{-}TiO_x$ system at 1873 K and $pO_2 = 10^{-12}$ atm, as measured by metal-slag-gas equilibrium experiments. Values shown are calculated averages from the 3 experimental series.

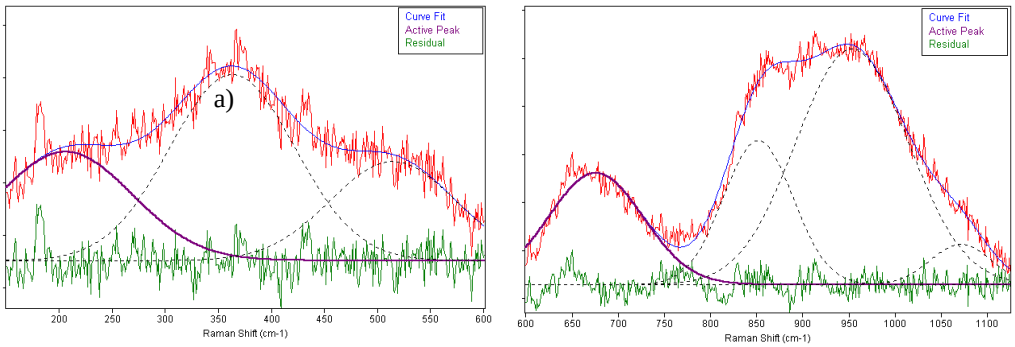

Figure 4: Raman Shift for a titanium free CaO-SiO_2 slag (CaO/SiO_2~1.25), equilibrated under air at 1873 K. **Left)** Low frequency envelope. **Right)** High frequency envelope

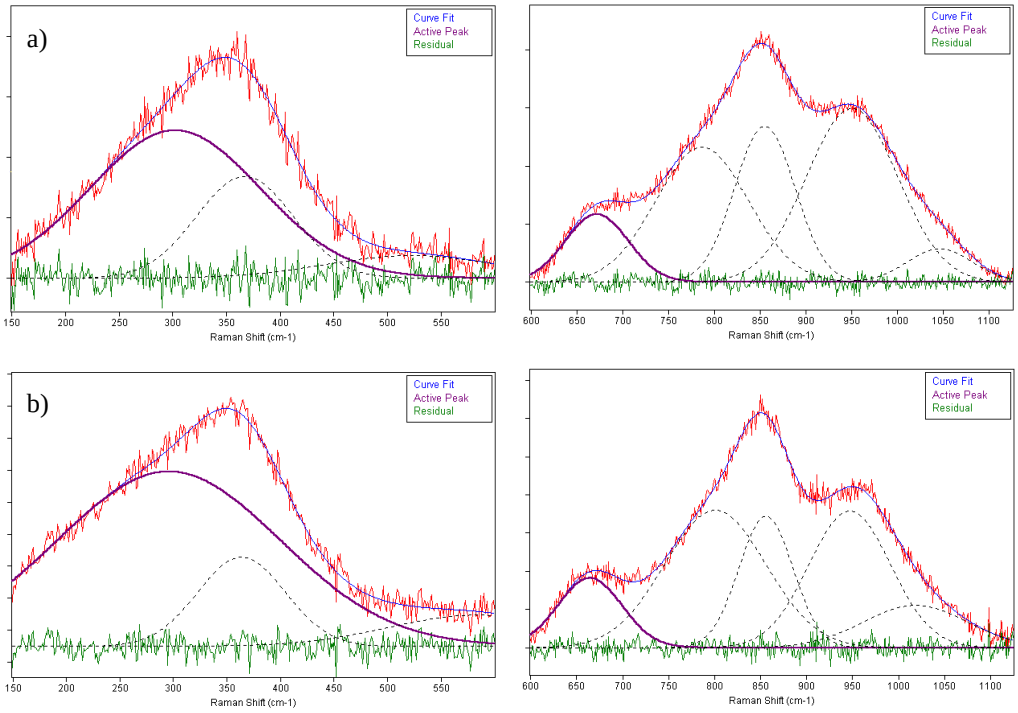

Figure 5: Raman Shift for slag 1 (CaO/SiO_2~1.25, 7 wt% TiO_x), equilibrated under **a)** air at 1873 **b)** under $pO_2 \sim 10^{-12}$ atm at 1873 K. Left - Low frequency envelope. Right - High frequency envelope

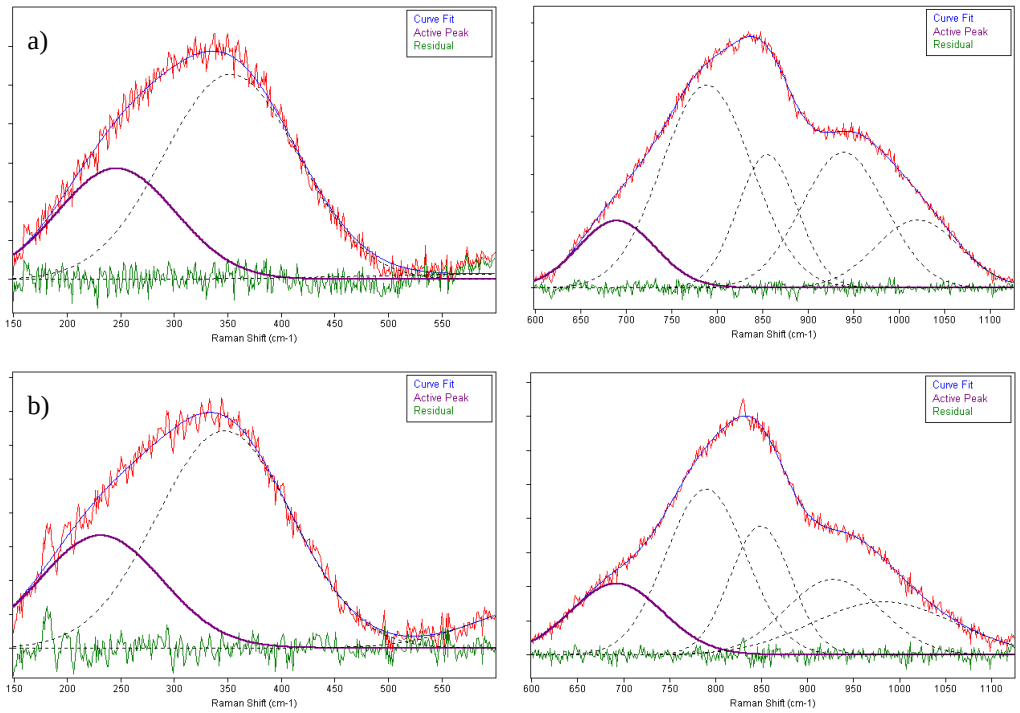

Figure 6: Raman Shift for slag 5 (CaO/SiO_2~1.25, 14 wt% TiO_x), equilibrated under **a)** air at 1873 **b)** under $pO_2 \sim 10^{-12}$ atm at 1873 K. Left - Low frequency envelope. Right - High frequency envelope

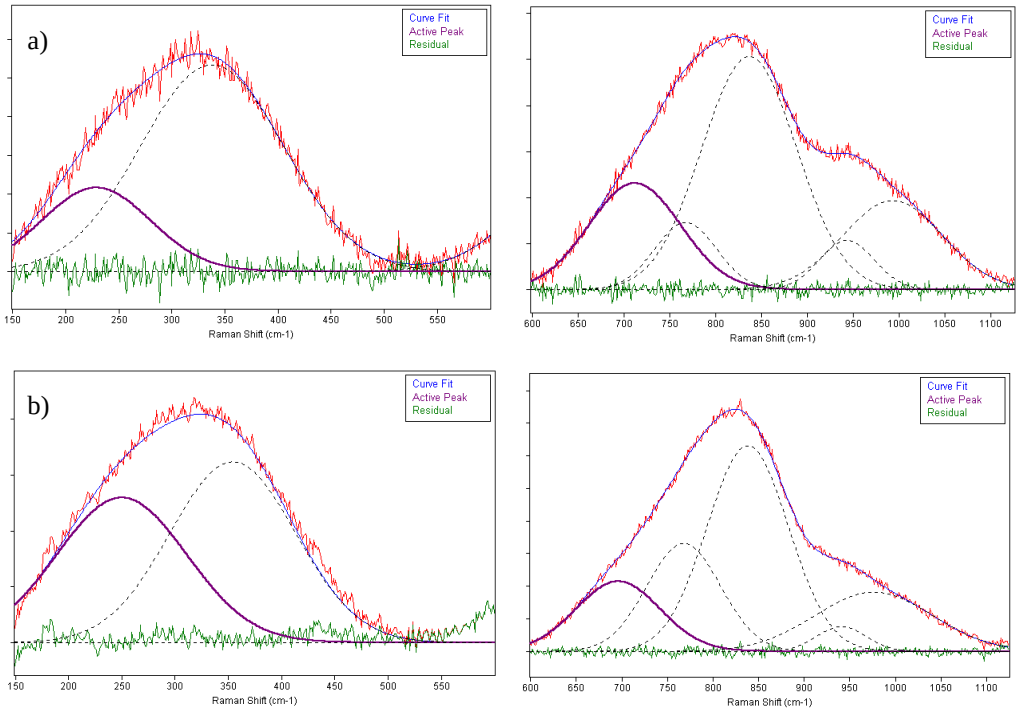

Figure 7: Raman Shift for slag 9 (CaO/SiO_2~1.25, 21 wt% TiO_x), equilibrated under **a)** air at 1873 **b)** under $pO_2 \sim 10^{-12}$ atm at 1873 K. Left - Low frequency envelope. Right - High frequency envelope.

Table I: Composition of master slags, as analysed by ICP-AES

Slag	CaO/SiO_2 (wt%)	TiO_2 (wt%)
1	1.25	7.30
2	0.99	7.55
3	0.77	7.78
4	0.53	7.34
5	1.21	14.40
6	1.00	14.20
7	0.70	14.60
8	0.56	14.80
9	1.21	20.85
10	1.00	22.00
11	0.75	22.20
12	0.56	21.70
13	1.35	52.35
14	1.00	51.10

Table II Results from the metal-slag-gas equilibrium experiments trial series, conducted in CO/CO_2 atmosphere at 1873 K, $CO/CO_2 = 456 \Rightarrow pO_2 = 10^{-12}$ atm. Equilibriation time 8 hours.

Slag No	Element Concentration in Copper						Metallic "Contamination" in Slag		Calculated Activities (γ_{Si} = 0.018)		Ti^{3+}/Ti^{4+} in Slag
	X_{Si} (wt ppm)		X_{Ti} (wt ppm)		X_{Mo} (wt ppm)		Cu (wt ppm)	Mo (wt ppm)	aSi (In Copper)	$aSiO_2$ (In Slag)	
8h	GDMS	ICP	GDMS	ICP	GDMS	ICP					
1	132.0	70	0.008	0.7	22.9	-	1104	51	4.11E-06	0.035	0.204
2	280.5	255	0.005	0.6	30.6	-	894	90	1.09E-05	0.093	0.303
3	247.5	245	0.003	0.1	26.6	-	1489	81	1.00E-05	0.086	0.455
4	225.5	240	0.002	0.1	28.3	-	1060	110	9.48E-06	0.081	0.632
5	71.5	65	0.002	0.2	25.5	-	950	68	2.78E-06	0.024	0.180
6	110.5	107	0.006	0.3	26.7	-	791	69	4.43E-06	0.038	0.218
7	286.5	295	0.006	0.2	30.2	-	884	77	1.18E-05	0.101	0.400
8	300.0	280	0.007	0.4	29.5	-	1276	120	1.18E-05	0.101	0.469
9	79.5	130	0.008	0.5	29.1	-	780	152	3.24E-06	0.028	0.189
10	149.5	160	0.003	0.3	24.3	-	1145	38	6.30E-06	0.054	0.242
11	321.8	290	0.007	0.4	25.6	-	1320	49	1.25E-05	0.106	0.413
12	328.0	290	0.050	0.3	27.2	-	1850	98	1.26E-05	0.107	0.516
Reference*	0.08	-	0.003	-	<0.008	-	-	-	-	-	-
1 (24h)	73	-	0.002	-	33	-	-	-	2.97E-06	0.025	0.176
2 (24h)	234	-	0.005	-	16.6	-	-	-	9.53E-06	0.081	0.242
5 (24h)	52	-	0.004	-	29	-	-	-	2.12E-06	0.018	0.140
6 (24h)	102	-	0.005	-	32	-	-	-	4.15E-06	0.035	0.220

*Analysis of the pure unreacted copper metal.

Table III Results from the metal-slag-gas equilibrium experiments first series, conducted in H_2/H_2O atmosphere at 1873 K. Equilibriation time 24 hours.

Slag No	Measured pO_2 (atm)	Element Concentration in Copper						Calculated Activities (γ_{Si} = 0.018)		Ti^{3+}/Ti^{4+} in Slag
		X_{Si} (wt ppm)		X_{Ti} (wt ppm)		X_{Mo} (wt ppm)		aSi (In Copper) (Average)	$aSiO_2$ (In Slag) (Average)	
24h		GDMS	ICP	GDMS	ICP	GDMS	ICP			
1	4.20E-12	29	27.9	0.07	5.47	185	212	1.18E-06	0.042	0.086
2	2.23E-11	69	91.8	0.18	0.06	120	200	2.81E-06	0.535	0.239
3	1.42E-11	124	103	0.32	0.77	97	183	5.05E-06	0.612	0.520
4	1.45E-11	233	106	0.02	0.36	94	196	9.49E-06	(1.175)	0.658
5	9.72E-12	46	34.1	0.13	0.13	133	171	1.87E-06	0.155	0.123
6	7.66E-12	*	85.5	*	0.68	*	216	3.48E-06	0.228	0.234
7	3.44E-12	*	224	*	0.67	*	202	9.12E-06	0.268	0.485
8	1.34E-11	*	251	*	0.68	*	237	1.02E-05	(1.170)	0.732
9	1.02E-12	68	28.9	0.95	109	504	330	2.77E-06	0.024	0.218
10	3.76E-12	90	60.6	0.13	0.54	90	159	3.67E-06	0.214	0.171
11	5.03E-12	197	71.8	0.38	1.61	500	258	8.02E-06	0.343	0.354
12	9.03E-12	310	84.1	0.8	3.62	162	196	1.26E-05	0.973	0.467
13	7.94E-13	805	118	0.15	10.1	205	291	3.28E-05	0.227	0.453
14	2.95E-12	374	91	0.08	3.31	179	322	1.52E-05	0.432	0.452

In cases where concentrations of Si in copper differ substantially between analysis methods, the largest of the two values was used for calculation

*Due to sample porosity, these samples could not be analysed with GDMS

Table IV Results from the metal-slag-gas equilibrium experiments secod series, conducted in H_2/H_2O atmosphere at 1873 K. Equilibriation time 24 hours.

Slag No	Measured pO_2(atm)**	Element Concentration in Copper						Calculated Activities (γ_{Si} = 0.018)		Ti^{3+}/Ti^{4+} in Slag
		X_{Si} (wt ppm)		X_{Ti} (wt ppm)		X_{Mo} (wt ppm)		aSi (In Copper)	$aSiO_2$ (In Slag)	
24h		GDMS	ICP	GDMS	ICP	GDMS	ICP			
1	5E-12	*	60	*	1.9	*	200	2.44E-06	0.104	0.092
2	5E-12	150	115	0.004	<0.5	34.2	200	5.40E-06	0.230	0.262
3	5E-12	148	130	0.006	<0.5	20.1	170	5.66E-06	0.242	0.530
4	5E-12	430	235	0.006	<0.5	24.4	131	1.35E-05	0.578	0.691
5	5E-12	64.9	55	0.006	<0.5	16.4	125	2.44E-06	0.104	0.101
6	5E-12	*	155	*	0.7	*	220	6.31E-06	0.270	0.283
7	5E-12	269	180	0.008	<0.5	17.5	165	9.14E-06	0.390	0.402
8	5E-12	420	310	0.03	0.9	24.3	190	1.49E-05	0.635	0.685
9	5E-12	114	90	0.03	0.6	24	210	4.15E-06	0.177	0.188
10	5E-12	*	70	*	12	*	230	2.85E-06	0.122	0.296
11	5E-12	356	240	0.07	0.7	32.9	180	1.21E-05	0.518	0.483
12	5E-12	526	355	0.06	1	56.1	415	1.79E-05	0.766	0.690
12(2h)	5E-12	*	180	*	1.4	*	185	-	-	0.567
12(6h)	5E-12	*	190	*	3.7	*	195	-	-	0.562
12(18h)	5E-12	*	360	*	2.3	*	170	-	-	0.568

*Due to sample porosity, these samples could not be analysed with GDMS

**Oxygen pressure measured in two samples to 5E-12 atm. Others approximated to the same

In cases where concentrations of Si in copper differ substantially between analysis methods, the largest of the two values was used for calculation